utilized to determine the velocity and concentration throughout the fluid. Solutions have been obtained for both constant wall composition and constant wall mass flux boundary conditions. The latter condition might be met in nature if low-density silicic melt is generated by partial fusion along the wall of the chamber. If this is to occur, however, large amounts of heat must be supplied to the chamber to offset the dissipated heat and the energy consumed in partial melting. A possible magmatic source of the necessary heat would be the repeated injection of primitive magma into the roots of the chamber[5,8,23,24]. The former condition ($C_w = $ const) could be attained if, for example, hydrous country rocks buffer the concentration of H_2O along the margins of the chamber[1].

The growth of a stratified layer at the top of a chamber is given by the rate at which buoyant melt crosses the plane $x = L - \Delta(t)$ (see Fig. 3). In Fig. 4, the rates of accumulation of evolved magma for various bulk compositions are plotted against mass diffusivity. The range of mass accumulation rates inferred from natural systems is also plotted. Figure 4 suggests that rates of marginal upwelling are too small by several orders of magnitude to explain gradients in SiO_2 as found in pyroclastic deposits. For H_2O, vertical stratification by the buoyant upwelling mechanism appears marginally possible. Additional calculations in which the variations of viscosity and D_{H_2O} with H_2O concentration are explicitly considered are in progress.

The critical thermal Rayleigh number for the onset of turbulence is a function of the fluid Prandtl number. Because of the lower Prandtl number, turbulent convection is more probable in basaltic, as opposed to rhyolitic, chambers. Within rheological and thermal boundary layers in non-isothermal chambers however, turbulence would be suppressed. In an isothermal chamber, turbulent boundary layers might develop in a basaltic chamber. Modification of results found in ref. 27 leads to an approximate expression for the mass flow ($\dot{M}$) in a chamber characterized by turbulent boundary layers. The magnitude of $\dot{M}$ is not very different than that in the laminar flow case. In addition, the effects of entrainment and mixing[28] are greater in the case of turbulence and so the composition of evolved melt delivered to the chamber roof would be less silicic.

In magma chambers, where thermal and chemical buoyancy effects are present, marginal velocities are dominated by downwelling effects for components with $Le > 10^6$. Rapidly diffusing components such as H_2O in low-viscosity, basaltic reservoirs may show countercurrent flow. Upflow is maximized in isothermal chambers; however, for species other than highly mobile ones ($D > 10^{-11} \text{ m}^2 \text{ s}^{-1}$) the upward mass flow rate through the chemical boundary layer is small compared with the inferred rate of roofward magma accumulation. In an isothermal chamber, the upflow mechanism is marginally feasible in generating roofward accumulations of magma zoned in H_2O; vertical zonation with respect to silica appears to be precluded, however.

1. Shaw, H. R. *Geochemical Transport and Kinetics*, 139–170 (Carnegie Institute of Washington, 1974).
2. Smith, R. L. *Geol. Soc. Am. Spec. Pap.* **180**, 5–28 (1979).
3. McBirney, A. R. *J. Volcan. Geotherm. Res.* **7**, 357–371 (1980).
4. Spera, F. J. & Crisp, J. A. *J. Volcan. Geotherm. Res.* **11**, 169–187 (1981).
5. Hildreth, W. *J. geophys. Res.* **11**, B11, 10153–10193 (1981).
6. Turner, J. S. & Gustafson, L. B. *J. Volcan. Geotherm. Res.* **11**, 93–125 (1981).
7. Smith, R. L. & Bailey, R. A. *Bull. volcan.* **29**, 83–104 (1966).
8. Spera, F. J., Yuen, D. A. & Kirschvink, S. J. *J. geophys. Res.* **87**, 8655–8667 (1982).
9. Whalen, J. B. *Geochim. cosmochim. Acta* **47**, 1443–1457 (1983).
10. Ludington, S. *J. geophys. Res.* 10423–10430 (1981).
11. Lesher, C. E., Wlker, D., Candela, P. & Hays, J. F. *Geol. Soc. Am. Abstr. Prog.* **14**, 545 (1982).
12. Schmincke, H.-U. *Geol. Soc. Am. Abstr. Prog., Cord. Sec.* 231–232 (1972).
13. Hildreth, E. W. *Geol. Soc. Am. Spec. Pap.* **180**, 43–75 (1979).
14. Chen. C. F. & Turner, J. S. *J. geophys. Res.* **85**, 2573–2593 (1980).
15. Turner, J. *Nature* **285**, 213–215 (1980).
16. Michael, P. J. *Geology* **11**, 31–34 (1983).
17. Nilson, R. H. & Baer, M. R. *Sandia National Laboratories Rep. SAND80-2397* (1981).
18. Yuen, D. A. & Schubert, G. *J. geophys. Res.* **81**, 2499–2510 (1976).
19. Carrigan, C. R. *J. Volcan. Geotherm. Res.* **16**, 279–298 (1983).
20. Turner, F. J. *Metamorphic Petrology* (McGraw-Hill, New York, 1968).
21. Kemp, D. thesis, Princeton Univ. (1984).
22. Morgan, G. W. & Warner, W. H. *J. aeronaut. Sci.* **23**, 937–948 (1956).
23. Huppert, H. E. & Sparks, R. S. *Contr. Miner. Petrol.* **75**, 279–289 (1980).
24. Hardee, H. C. *Bull. volcan.* **45–1**, 42–49 (1982).
25. Hieber, C. A. & Gebhart, B. *J. Fluid. Mech.* **49**, 577–591 (1971).
26. Golitsyn, G. S. *J. Fluid Mech.* **95**, 567–608 (1979).
27. Eckert, E. G. & Jackson, T. W. *Rep. Nat. Adv. Comm. Aero. Tech. Not.* 2207 (1950).
28. Olson, P. M., Yuen, D. A. & Balsinger, D. S. *J. geophys. Res.* **89**, 425–436 (1984).
29. Delaney, J. R. & Karsten, J. L. *Earth planet. Sci. Lett.* **52**, 191–202 (1981).
30. Watson, E. B. *Contr. Miner. Petrol.* **80**, 73–87 (1984).
31. Alibert, C. & Carron, J. P. *Earth planet. Sci. Lett.* **47**, 294–306 (1980).
32. Hart, S. R. *Geochim. cosmochim. Acta* **45**, 279–291 (1981).
33. Bottinga, Y., Richet, P. & Weill, D. F. *Geochim. cosmochim. Acta* **46**, 909–919 (1982).
34. Burnham, C. W. & Davis, N. F. *Am. J. Sci.* **270**, 54–79 (1971).
35. Bottinga, Y., Weill, D. F. & Richet, P. *Bull. Miner.* **106**, 129–138 (1983).
36. Dowty, E. & Berkebile, C. A. *Am. Miner.* **67**, 900–906 (1982).
37. Powell, M. A., Walker, D., Grove, T. L. & Hays, J. F. *Geol. Soc. Am. Abstr. Prog.* **12**, 502 (1980).
38. Murase, T. & McBirney, A. R. *Bull. geol. Soc. Am.* **84**, 3563–3592 (1973).
39. Carmichael, I. S. E., Nicholls, J., Spera, F. J., Wood, B. J. & Nelson, S. A. *Phil. Trans. R. Soc. A* **286**, 373–431 (1977).

Cause and implications of rock varnish microchemical laminations

Ronald I. Dorn

Department of Geography, University of California, Los Angeles, California 90024, USA

Rock varnish is a dark coating composed mostly of clays and manganese and iron oxides[1] that accretes on rock surfaces in all terrestrial environments[2]. Perry and Adams[3] first observed micronscale manganese-rich and manganese-poor (relatively iron-rich) layers in varnish and proposed that these may be related to unspecified environmental changes. Electron microprobe analyses reported here suggest that Mn:Fe ratios vary systematically with depth in varnishes on K/Ar-dated volcanic rocks from the Coso and Cima volcanic fields, eastern California, and on talus flatirons in the Negev Desert, Israel. These microchemical laminations probably reflect past fluctuations in the level of aeolian alkalinity, and possibly climatic change. This new indicator of terrestrial environmental change may be of importance to research on geomorphology, archaeology, palaeoclimatology, and Quaternary studies in arid environments.

Several lines of evidence support the premise that alternating manganese-poor and manganese-rich laminae in varnish on subaerial exposed rock surfaces are linked to the alkalinity of the aeolian environment. (1) The manganese-oxidizing microorganisms that are probably responsible for manganese enhancement in varnish[2,4] are inhibited by alkalinity[4–6]. (2) If manganese concentration occurs by a physicochemical fractionation process[7,8], where manganese is mobilized from ambient material and fixed in varnish under slight pH-Eh fluctuations and iron is not, a lack of periodic fluctuations to slightly more acidic conditions in a geochemical regime that is highly alkaline could also promote a varnish poor in manganese. (3) Except for acid springs and acid mine-drainages where iron is fixed by chemolithotrophic bacteria[9], orange (manganese-poor) varnishes only occur in deserts where rock surfaces are in constant, direct contact with alkaline material. In contrast, manganese-rich (black) varnishes have been observed in all terrestrial weathering environments that are not acidic enough to mobilize manganese from surficial coatings[2]. (4) Contemporary manganese-rich varnishes have near-neutral pH values, and manganese-poor varnishes have alkaline pH levels[10].

However, several potential sources of error may confuse this assumed relation between varnish microchemical laminations and regional alkalinity levels. (1) Dominant local influences could interfere with a regional signal. For instance, accumulation of organic material from adjacent plants or airborne fallout from a nearby deflation surface could inhibit manganese oxidation by microorganisms. (2) Microlaminations are usually discontinuous from microdepression to microridge (on a millimetre to centimetre scale), and they can sometimes be discontinuous within the same microdepression. These discontinuities may be caused by differential rates of varnish accumulation, differential compression of subsurface varnish, anomalous alkaline detritus (see Fig. 2b in ref. 10), and/or localized chemical or mechanical

erosion of varnish. (3) Manganese-poor layers could represent periods when manganese is leached, leaving an iron-rich lag[2,8]. However, Perry and Adams[3] and Elvidge and Iverson[7] feel that laminations are primary depositional features, and an erosional cause has also been disputed[2]. First, the surface layers of varnish in less arid environments (more chemically erosive to manganese) are manganese-rich, whereas varnishes with iron-

rich surface layers are found in alkaline, hyper-arid environments. Second, although microenvironmental variations between microdepressions and microridges can cause discontinuities in laminations, it is less likely that a major climatic change would be as discriminating. (4) In rock crevices in arid environments, orange (manganese-poor) varnish often develops in direct contact with alkaline desert dust. With spalling, this
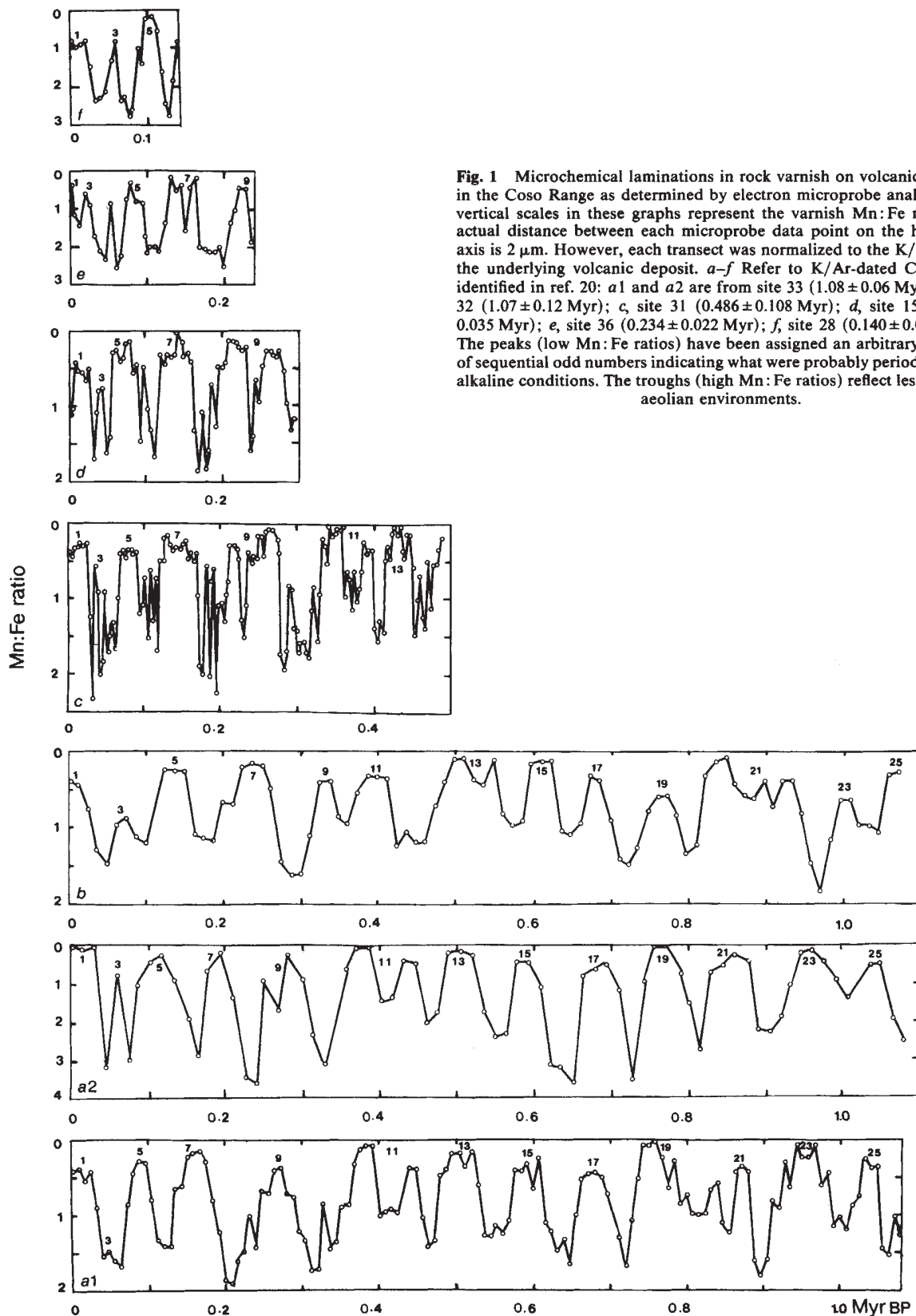
Fig. 1 Microchemical laminations in rock varnish on volcanic deposits in the Coso Range as determined by electron microprobe analyses. The vertical scales in these graphs represent the varnish Mn:Fe ratio. The actual distance between each microprobe data point on the horizontal axis is 2 μm. However, each transect was normalized to the K/Ar-age of the underlying volcanic deposit. a-f Refer to K/Ar-dated Coso sites, identified in ref. 20: a1 and a2 are from site 33 (1.08 ± 0.06 Myr); b, site 32 (1.07 ± 0.12 Myr); c, site 31 (0.486 ± 0.108 Myr); d, site 15 (0.293 ± 0.035 Myr); e, site 36 (0.234 ± 0.022 Myr); f, site 28 (0.140 ± 0.089 Myr). The peaks (low Mn:Fe ratios) have been assigned an arbitrary notation of sequential odd numbers indicating what were probably periods of more alkaline conditions. The troughs (high Mn:Fe ratios) reflect less-alkaline aeolian environments.

crack varnish is exposed to less-alkaline, subaerial conditions and subsequently receives a superposed layer of black varnish enriched in manganese. Thus a basal sequence of manganese-poor under manganese-rich varnish may not reflect fluctuations in the alkalinity of aeolian fallout. (5) Some varnishes have microprobe Mn:Fe profiles that reveal no laminations. This may be due to improper thin-section preparation, varnish accretion rates that are too slow to record these environmental changes, or environments that do not experience significant fluctuations in alkalinity.

To assess the consistency and significance of Mn:Fe microchemical laminations, varnishes were sampled from the surfaces of 11 K/Ar-dated rhyolite domes and south to south-west facing basalt flows in the Coso Range, eastern California. Because the focus of this study is on the sensitivity of varnish to regional fluctuations in levels of aeolian alkalinity, varnish samples were only collected from the tops of rock exposures at least 1 m above adjacent soil surfaces.

Figure 1 presents electron microprobe transects from the varnish surface to the underlying rock, each representative of multiple microprobe transects of the varnish analysed from six of the volcanic flows. Varnishes of five other volcanic deposits in the Coso Range were analysed and not reported here, but microprobe analyses reveal very similar results (R.I.D., in preparation). Successive microprobe analyses were taken at 2-μm intervals. For ease of comparison, varnish depths were normalized to the K/Ar-age of the underlying deposits. Note that the time intervals in Fig. 1 are only approximations, because: (1) although the rate of varnish accretion was assumed to be constant for the construction of Fig. 1, this rate probably varies; (2) different time lags may occur between exposure of a surface to the subaerial environment and the onset of varnishing; (3) significant age-uncertainties are assigned to some of the K/Ar-dated volcanic flows, and (4) compression of older varnish probably occurs after burial.

Multiple microprobe transects were made into varnishes on several rocks from each of the 11 Coso flows. a1 and a2 in Fig. 1 exemplify variations that can be found in transects from adjacent rocks in the same volcanic flow. The most consistent results occurred in 1-3 mm-wide microdepressions collected from sloping surfaces. The average rate of varnish accretion in these small hollows is probably rapid enough to record major fluctuations in regional levels of alkaline aerosols, and these microdepressions are probably too small to generate their own microenvironment. About one-third of the transects had discontinuous microlaminations or profiles with few or no variations
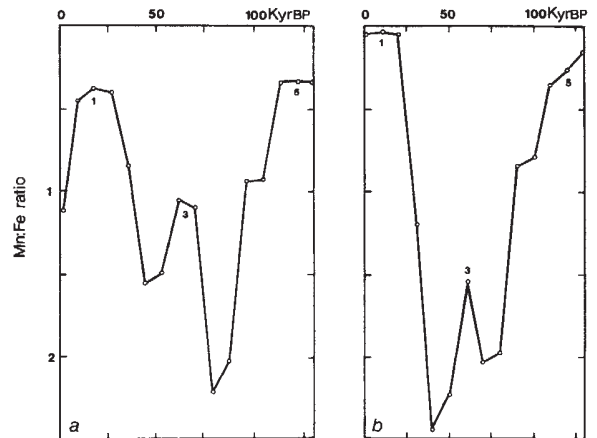

Fig. 2 Microchemical laminations of varnish on Cima basalt flow i_2 (K/Ar-age of 0.13 ± 0.06 Myr)[11]. a and b are transects from two separate rock exposures.

in Mn:Fe ratios. The remainder are continuous and fairly consistent, including the microchemical laminations presented in Fig. 1.

Figure 2 presents microprobe transects from rock varnish on two separate rock outcrops on a 130,000 + 60,000 BP K/Ar-dated basalt flow in the Cima volcanic field of eastern California[11]. Like the Coso Range, varnish on the Cima basalt flow was collected from constructional surfaces. The sequence of high and low Mn:Fe ratios in the Cima varnish is remarkably similar to the sequence of Mn:Fe rations from the Coso Range over the same approximate time period.

Figure 3 illustrates the microlaminations of varnishes on talus flatirons in the Negev Desert of Israel. Gerson[12] proposed a climatic–geomorphic model for the development of sequences of inset flatirons, where talus is built up in lengthy, more humid periods and eroded during arid phases of long duration. According to Gerson's model the varnishes on the oldest of three talus flatirons should have experienced three major arid periods separated by two long humid periods. This is indeed reflected in microprobe transects of varnish on the oldest flatiron at two localities in the Negev Desert (Fig. 3). The low Mn:Fe ratio of the basal layer may represent varnishing during an arid-alkaline phase after the humid period when the talus was deposited. Above this iron-rich band are two cycles of manganese-rich and
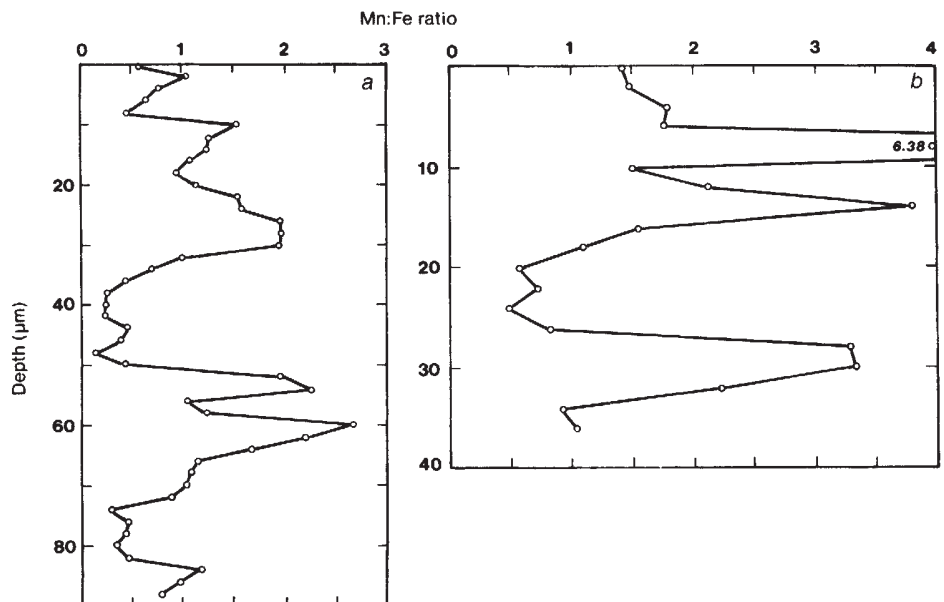

Fig. 3 Microprobe profiles of varnish collected from the oldest flatiron in sequences of inset talus flatirons in the Negev Desert, Israel. a, Representative transect of varnish on syenite in the Timna Valley, southern Negev. More humid periods are interpreted as occurring from ~8–34 μm and from ~50–70 μm. b, Representative transect of varnish on chert near Paran in the Arava Valley, central Negev. More humid phases are likely from ~6–16 μm and from ~26–34 μm. Because no absolute age-estimates are available, the depth from the surface to the underlying rock is plotted against the Mn:Fe ratio.

manganese-poor laminations, corresponding with the development of the two younger talus flatirons at each site. Microprobe analyses of varnishes on the younger flatirons are also consistent with Gerson's model (R.I.D., in preparation).

The consistency of these preliminary results warrant some tentative interpretations. The sites reported here are adjacent to basins that have alternated between pluvial lakes and saline playas during the Quaternary[13-15]. Similarly, when these lakes were present, the vegetative cover was probably more extensive[16-18]. During presumably warmer-drier climates, saline playas developed and the vegetation cover over desert soils decreased, providing a more abundant source of alkaline aerosols[19] that probably fell on neighbouring upland areas. Thus, the climate of these areas may have controlled fluctuations in the concentrations of alkaline aeolian fallout and hence influenced Mn:Fe ratios in varnishes. High ratios probably reflect less alkaline conditions, and low ratios probably indicate more alkaline conditions. The sensitivity of varnish Mn:Fe ratios to fluctuations in alkalinity appears to be of the order of 10,000–25,000 yr and is probably dependent on the rate of varnish accretion.

Note that each individual microprobe transect only reflects the history of influences imposed on that given rock. Systematic sets of intra-rock, inter-rock, and inter-site transects of microchemical laminations are required before a record of regional changes in the aeolian fallout can be reasonably interpreted. These have been obtained for the Coso Range (R.I.D., in preparation), although more extensive microprobe work is still required to determine conclusively under what conditions uniform lamination sequences develop. The offsets that do occur between the varnish profiles in Fig. 1 may result from: differences in the time required to initiate varnishing on the volcanic deposits; uncertainty in the K/Ar-ages; variable rates of varnish accretion, and differential compression, particularly with respect to the most recent peak of low Mn:Fe ratios. This most recent peak, labelled as stage 1, lacks the compression that is likely to occur in older varnish after burial. The greater relative length of stage 1 may also in part be due to the possible attenuation of this surficial layer of varnish during thin section preparation, and a faster rate of clay accumulation during the Holocene and similar environments.

Over approximately the past million years in the Coso Range, eastern California, there have been systematic fluctuations in rock varnish Mn:Fe ratios that probably reflect variations in regional aeolian alkalinity and possibly changes in climate. These rock varnish microchemical laminations are also documented in the Mojave Desert of eastern California and in the Negev Desert of Israel. However, before microchemical laminations can be interpreted reliably as a record of fluctuations in alkaline aeolian fallout, more data are needed to establish conclusively the link between Mn:Fe ratios and alkaline aeolian fallout and to assess the factors that influence inconsistencies in rock varnish microchemical laminations. This new record of terrestrial environmental change during the Quaternary is speculative, but it has considerable potential as a long-term indicator of past climates and as a tool to correlate landforms in what are at present arid lands.

1. Potter, R. & Rossman, G. R. Chem. Geol. 25, 79–94 (1979).
2. Dorn, R. I. & Oberlander, T. M. Prog. Phys. Geogr. 6, 317–367 (1982).
3. Perry, R. & Adams, J. Nature 276, 489–491 (1978).
4. Dorn, R. I. & Oberlander, T. M. Science 213, 1245–1247 (1981).
5. Schweisfurth, R., Jung, W. & Jacobs, M. in Geology and Geochemistry of Manganese, Volume 3. (eds Varentsov, I. M. & Grassely, Gy.) 279–283 (E. Schweizerbart'sche, Stuttgart, 1980).
6. Bromfield, S. M. & David, D. J. Soil Biol. Biochem. 8, 37–43 (1976).
7. Elvidge, C. D. & Iverson, R. M. in Environmental Effects of Off Road Vehicles (eds Webb, R. J. & Wilshire, H. G.) 225–243 (Springer, New York, 1983).
8. Whalley, W. B. in Chemical Sedimentation and Geomorphology (eds. Goudie, A. & Pye, K.) 197–226 (Academic, London, 1983).
9. Mallard, G. E. U.S. geol. Surv. Circ. 848-E, E13–E21 (1981).
10. Dorn, R. I. Quat. Res. 20, 49–73 (1983).
11. Dohrenwend, J. C., McFadden, L. D., Turrin, B. D., & Wells, S. G. Geology 12, 163–167 (1984).
12. Gerson, R. Israel J. Earth Sci. 31, 123–132 (1982).
13. Smith, G. I., Barczak, V. J., Moulton, G. F. & Liddicoat, J. C. U.S. geol. Surv. Prof. Pap. No. 1256 (1983).
14. Ore, H. T. & Warren, C. N. Bull. geol. Soc. Am. 82, 2553–2562 (1971).
15. Begin, Z. B., Ehrlich, A. & Nathan, Y. Israel geol. Surv. Bull. No. 63 (1974).
16. Spaulding, W. G., Leopold, E. B. & Van Devender, T. R. in Late Quaternary Environment of the United States. Vol. 1, The Late Pleistocene (ed. Porter, S. C.) 259–293 (University of Minnesota Press, Minneapolis, 1983).
17. Wells, P. V. Ecol. Monogr. 53, 341–382 (1983).
18. Mehringer, P. J. in Models and Great Basin Prehistory (ed. Fowler, D.) 113–167 (Desert Research Institute, Reno and Las Vegas, 1977).
19. McFadden, L. D., Dohrenwend, J. C. & Wells, S. G. in Surficial Geology of the Eastern Mojave Desert Region (ed. Dohrenwend, J. C.) (Geological Society of America Annual Meeting Guidebook, Reno, in the press.)
20. Duffield, W. A. & Bacon C. R. U.S. geol. Surv. Misc. Invest. Map I-1200 (1981).

Dimethyl sulphide in a stratified coastal salt pond

Stuart G. Wakeham*, Brian L. Howes†
& John W. H. Dacey†

* Department of Chemistry, and † Department of Biology,
Woods Hole Oceanographic Institution, Woods Hole,
Massachusetts 02543, USA

Dimethyl sulphide (DMS) is the major volatile reduced organic sulphur compound in open ocean and coastal waters, and its emission from surface water represents a major flux of biogenic reduced sulphur to the atmosphere[1-8]. It is an algal natural product[4,9-11] as well as a product of microbial decomposition of organic matter[12-15]. In the open ocean, the distribution of DMS is correlated with primary productivity[3,4,6,8]. In a study of a stratified coastal salt pond reported here, DMS was the predominant volatile sulphur compound in the oxic epilimnion throughout the year. There was consistently a peak in DMS concentration just above the oxic–anoxic interface at low oxygen tensions, probably arising from a combination of physiological stress and decomposition of algal material. During winter and early spring, a second DMS peak was present in the epilimnion, probably associated with algal production. Elevated DMS concentrations did not seem to be related to strict anoxia, as the lowest concentrations were always found in the anoxic hypolimnion where H_2S (a volatile reduced inorganic sulphur compound) dominates.

Salt Pond is a shallow (5.5-m deep) eutrophic marine basin on Cape Cod, Massachusetts[16], that exhibits density stratification. While aerobic processes dominate the epilimnion, the anaerobic hypolimnion generally has high concentrations of H_2S (up to ~5 mM) generated from sulphate reduction in the bottom waters and sediments. In summer, the anoxic zone rises to within 2–3 m of the pond surface and the oxic–anoxic interface becomes quite pronounced, resulting in steep geochemical gradients. During winter, the depth of the interface deepens and H_2S concentrations decrease as a result of wind-driven mixing. Occasionally the water column overturns.

DMS concentrations were measured in the water column of Salt Pond between June 1982 and July 1983. Water samples were collected along a vertical profile in the central basin using a battery-operated peristaltic pump and a weighted silicon rubber tube[17] lowered sequentially to the appropriate sampling depths. Glass sample bottles (2 l) were rinsed, filled and stoppered without headspace. The water samples were returned to the laboratory within ~1 h of collection and were syringe-filtered through 0.22-μm Millipore filters to remove algal cells and poisoned with $HgCl_2$. $HgCl_2$ acted both to preserve the samples and to precipitate H_2S which, when present at high concentrations, interferes with our DMS assay. Volatile compounds were collected from the water subsamples (50–200 ml) by sparging